ELSEVIER

Journal of Molecular Structure: THEOCHEM 816 (2007) 59–65

THEO CHEM

www.elsevier.com/locate/theochem

Planar tetra-coordinate Si and Ge in perfectly squared Ni_4Cl_4X complexes

Jin-Chang Guo, Si-Dian Li *

Institute of Molecular Science, Shanxi University, Taiyuan 030001, Shanxi, PR China
Institute of Materials Science and Department of Chemistry, Xinzhou Teachers' University, Xinzhou 034000, Shanxi, PR China

Received 3 March 2007; received in revised form 29 March 2007; accepted 30 March 2007
Available online 13 April 2007

Abstract

Density functional theory investigations performed in this work indicate that planar tetra-coordinate silicon and germanium can be stabilized at the centers of the perfectly squared M_4Cl_4 ligands to form D_{4h} M_4Cl_4X complexes (M = Ni, Pd, Pt; X = Si, Ge). M_4Cl_4 ligands prove to be flexible enough to host other planar or quasi-planar tetra-coordinate inorganic atoms including C, B, Al, Ga, N, P, and As. Delocalized δ, π, and σ molecular orbitals are found to play important roles in stabilizing these novel structures. The ionization potentials of the neutrals and first vertical electron detachment energies of the anions have also been calculated to facilitate future experiments. The results obtained in this work complete the series of planar coordinate silicon and germanium with the highest symmetries of D_{4h}, D_{5h}, and D_{6h} in M_nN_nX series (M = transition metals; N = H, Cl; $n = 4, 5, 6$).

Keywords: Planar tetra-coordinate silicon; Density functional theory; Geometrical structures; Electronic structures

1. Introduction

Considerable progresses have been achieved in both theoretical and experimental investigations on planar tetra-coordinate carbon (ptC) since the concept was firstly proposed by Hoffmann and co-workers in 1970 [1–13]. Photoelectron spectroscopy investigations by Wang's group identified the smallest species of D_{4h} Al_4C^{2-} which contains a ptC at the center of the dianion in 1999 [2]. Planar penta-, hexa-, and hepta-coordinated carbons were designed later by Schleyer's group at density functional theory (DFT) level [14,15]. In two recent papers, our group presented a new approach to host ptC centers in the perfect squares of D_{4h} Ni_4H_4C and analogues [11,12]. In these complexes, transition metals function as ligands to ptC centers and H atoms serve as bridges between neighboring transition-metal atoms. PtC centers can also be stabilized by four-membered ring perimeters in naked $Cu_4C^{2+}$and its analogues [13].

Silicon lies directly under carbon in the same column of the periodic table and has a similar valence orbital configuration ($3s^2 3p^2$) with carbon ($2s^2 2p^2$). But it almost doubles carbon in sizes. This situation requires a much bigger cavity to geometrically fit a planar coordinate silicon than that to host a planar coordinate carbon. The existence of planar tetra-coordinate silicon (ptSi) with the symmetry of D_{2h} was firstly recognized about 30 years ago in orthosilicic acid ester [16] and C_{2v} ptSi and C_{2v} ptGe were recently observed in pentaatomic MAl_4^- anions in gas phases (M = Si and Ge) [17]. DFT investigations indicate that the most stable isomer of $Si(CO)_4$ contains a D_{2h} ptSi center [18]. Our group recently proposed a general pattern for planar tetra-, penta-, hexa-, hepta-, and octa-coordiante silicon [19,20]. We also designed planar penta-coordinate silicon (ppSi) in the perfect pentagons of D_{5h} M_5H_5Si (M = Ag, Au, Pd, Pt) [21] and planar hexa-coordinate

* Corresponding author. Address: Institute of Materials Science and Department of Chemistry, Xinzhou Teachers' University, Xinzhou 034000, Shanxi, PR China. Tel.: +86 0350 3048202; fax: +86 0350 3031845.
E-mail address: lisidian@yahoo.com (S.-D. Li).

0166-1280/$ - see front matter © 2007 Elsevier B.V. All rights reserved.
doi:10.1016/j.theochem.2007.03.040

silicon (phSi) in the perfect hexagon of D_{6h} Cu_6H_6Si [22]. However, to the best of our knowledge, there have been no systems containing ptSi centers with the highest symmetry of D_{4h} reported to date. In most reported systems, C_{2v} ptSi centers on the perimeters of fan-shaped structures have been confined within half-planes [17,19,20]. This causes considerable strains to destabilize the systems. It is anticipated that a D_{4h} ptSi at the center of a perfect square would be more feasible in energy. Considering the obvious electronic similarity and geometrical difference between Si and C, in this work, we replace H bridges with Cl in D_{4h} Ni_4H_4 to increase the cavity of the squared ligand, while keeping the four transition-metal atoms unchanged to fit a D_{4h} ptSi center. In this strategy, we have developed a new series of perfectly squared M_4Cl_4Si complexes (M = Ni, Pd, Pt) with the highest symmetry of D_{4h} which fit ptSi centers both electronically and geometrically. In these complexes, transition metals M serve as ligands to ptSi centers and Cl atoms function as bridges between neighboring transition-metal atoms. The cavities of D_{4h} M_4Cl_4 ligands turn out to be flexible enough to host various planar tetra-coordinate inorganic atoms at the centers, including C, Si, Ge, B, Al, Ga, N, P, and As. This provides a general pattern to host planar tetra-coordinate inorganic centers with the highest symmetry of D_{4h}. The results obtained in this work complete the series of the much concerned planar coordinate silicons with the highest symmetries of D_{4h}, D_{5h}, and D_{6h} in M_nN_nSi complex series (M = transition metals; N = H, Cl; $n = 4, 5, 6$).

2. Computational procedure

To parallel the results previously obtained for D_{5h} ppSi [21] and D_{6h} phSi [22], geometry optimizations, frequency analyses, and natural bonding orbital (NBO) analyses in this work were performed with the same hybridized procedure of DFT-B3LYP [23] implemented in Gaussian 03 program [24]. For systems containing the first-row transition metals, the basis of 6-311 + G(3df) was employed for all the component atoms. For the second- and third-row transition-metal complexes, the basis of 6-311 + G(d) was used for non-metal atoms and Lanl2dz for heavy transition metals (Lanl2dz contains an effective core potential for transition metals) [25]. The out valence Green function (OVGF) method [26] with the same bases was utilized to predict the ionization potentials (IPs) of the neutrals and the first vertical detachment energies (VDEs) of the anions. Fig. 1 depicts the optimized singlet structures of D_{4h} Ni_4Cl_4Si (**3**) and D_{2h} $Ni_6Cl_6Si_2$ (**4**) compared with that of the triplet D_{4h} Ni_4Cl_4 (**1**) and singlet D_{2d} Ni_4Cl_4 (**2**). Fig. 2 shows the low-lying isomers of Ni_4Cl_4Si with energies relative to the ground-state of D_{4h} Ni_4Cl_4Si (**3**) indicated. Fig. 3 compares the lowest unoccupied molecular orbital (LUMO), highest occupied molecular orbital (HOMO), and typical delocalized δ, π, and σ molecular orbitals (MOs) of D_{4h} Ni_4Cl_4Si (a) and D_{4h} Ni_4H_4C (b). The predicted infrared (IR) spectra of Ni_4Cl_4Ge, Ni_4Cl_4Si, and Ni_4Cl_4C are compared in Fig. 4 to facilitate future experiments. The calculated bond lengths, lowest vibration frequencies, HOMO energies, HOMO–LUMO energy gaps, the total Wiberg bond indices (WBIs) and natural atomic charges of the central atoms X, and the IPs of the neutrals and VDEs of the anions of the Ni_4Cl_4X complex series (X = C, Si, Ge, B, Al, Ga, N, P, As) are summarized in Table 1. Table 2 tabulates the corresponding results obtained for the second- and third-row transition-metal complex neutrals M_4Cl_4X (M = Pd, Pt; X = C, Si, Ge). Detailed DFT structures of all concerned neutrals and ions and the valence MO pictures of D_{4h} Ni_4Cl_4, D_{4h} Ni_4Cl_4Si, D_{4h} Ni_4Cl_4C, and D_{4h} Ni_4H_4C have been collectively tabulated in Supporting Information.

3. Results and discussions

As shown in Fig. 1 and Table 1, the perfectly squared triplet D_{4h} Ni_4Cl_4 ligand (**1**) with $r_{Ni-Ni} = 2.343$ Å and $r_{Ni-Cl} = 2.146$ Å is a true minimum with the lowest harmonic vibrational frequency of 12 cm^{-1} (b_{2u} mode). The singlet D_{2d} structure (**2**), in which the Ni_4 central square is well maintained while the four Cl atoms are off-planed, lies 0.70 eV above structure **3**. Introduction of a Si atom at the center of D_{4h} Ni_4Cl_4 produces the perfectly squared D_{4h} Ni_4Cl_4Si (**3**) which has the inter-atomic distances of $r_{Si-Ni} = 2.129$ Å, $r_{Ni-Ni} = 3.010$ Å, and $r_{Ni-Cl} = 2.192$ Å. Although the Ni_4 central square has been considerably expanded with a D_{4h} ptSi inside at the center, the Ni–Cl bridging bond lengths are kept practically the same throughout the whole Ni_4Cl_4X series with $r_{Ni-Cl} = 2.186$–2.209 Å. These values are very close to the corresponding bond length of $r_{Ni-Cl} = 2.146$ Å in D_{4h} Ni_4Cl_4 and $r_{Ni-Cl} =$

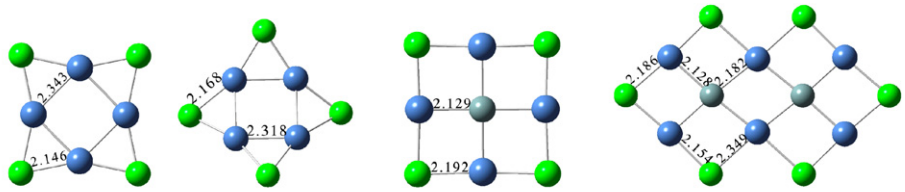

1. D_{4h} $Ni_4Cl_4(^3A_{1g})$ **2**. D_{2d} $Ni_4Cl_4(^1A_1)$ **3**. D_{4h} Ni_4Cl_4Si ($^1A_{1g}$) **4**. D_{2h} $Ni_6Cl_6Si_2$ (^1A_g)

Fig. 1. Optimized structures of singlet D_{4h} Ni_4Cl_4Si and D_{2h} $Ni_6Cl_6Si_2$ compared with triplet D_{4h} Ni_4Cl_4 and singlet D_{2d} Ni_4Cl_4 with necessary bond lengths indicated in Å.

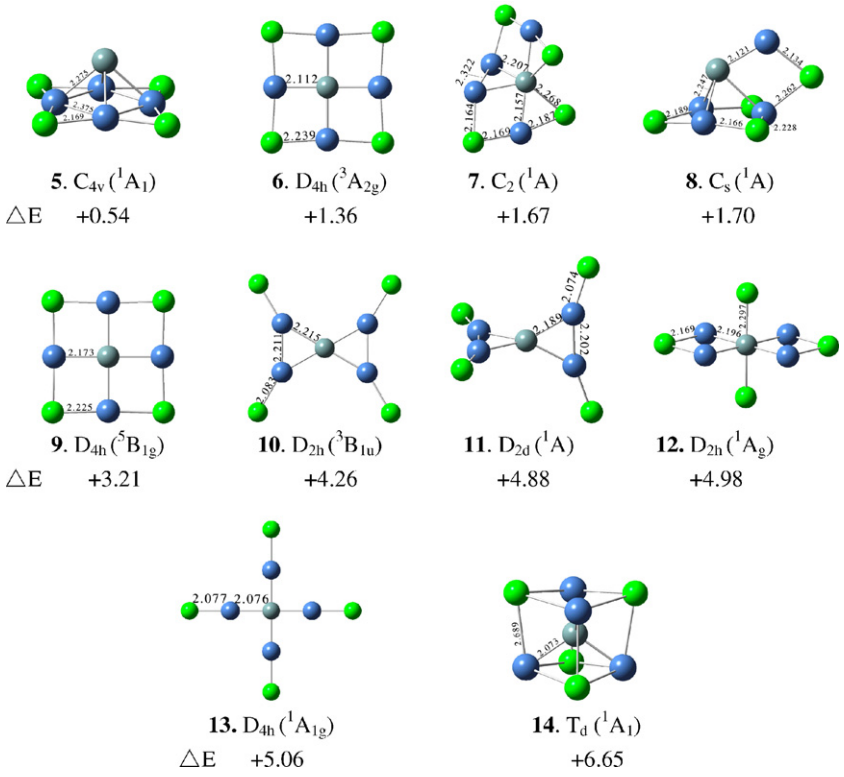

Fig. 2. Low-lying isomers of Ni_4Cl_4Si neutrals with energies relative to D_{4h} Ni_4Cl_4Si (**3**) indicated in eV.

2.168 Å in D_{2d} Ni_4Cl_4. As first-row main group atoms are much smaller than Si in size, insertion of a B, C, or N atom at the center of D_{4h} Ni_4Cl_4 only slightly elongates the Ni–Ni bonds (see Table 1). In fact, all group III, IV, and V atoms in the periodic table can be stabilized at the centers of Ni_4Cl_4, Pd_4Cl_4, and Pt_4Cl_4 squares to form planar or quasi-planar M_4Cl_4X complexes (see Tables 1 and 2). Most of these complexes possess the highest symmetry of D_{4h}, except for C_{2v} $Ni_4Cl_4N^+$, D_{2d} Pt_4Cl_4C, and D_{2d} Pt_4Cl_4Si which are slightly distorted to lower symmetries. The perfectly squared M_4Cl_4 transition-metal ligands (M = Ni, Pd, Pt) prove to be flexible enough to host various kinds of inorganic centers. These ligands share the same symmetry with D_{4h} Ni_4H_4 (D_{4h}) [11], but possess considerably longer bridging bond lengths ($r_{M-Cl} \approx 2.145$–2.398 Å) than $r_{Ni-H} = 1.613$ Å in Ni_4H_4. The obvious bond length increases and the deformable —Ni—Cl—Ni— bond angles introduce more flexibility to M_4Cl_4 ligands to host big inorganic centers like Si and Ge, while Ni_4H_4 can only geometrically fit the much smaller first-row inorganic centers including B, C, N, and O [11].

Various isomers of Ni_4Cl_4Si have been tested and compared with the D_{4h} ground-state structure (**3**). As indicated in Fig. 2, the second lowest-lying C_{4v} singlet isomer (**5**) lies 0.54 eV higher in energy than **3** and the D_{4h} triplet isomer (**6**) is 1.36 eV less stable. The much concerned tetrahedral arrangement of T_d **14** (an eighth-order saddle point) and D_{2d} **11** (a forth-order saddle point) turn out to lie much higher in energies (6.65 and 4.88 eV higher than **3**, respectively) and all the other 2D and 3D structures appear to be considerably less stable than **3**. Extensive searches produced no structures with lower energies. The lowest-lying isomer of D_{4h} Ni_4Cl_4Si (**3**) obtained in this work contains the first D_{4h} ptSi center in planar tetra-coordinate silicons reported so far [16–22] and competes the D_{nh} series of planar coordinate silicon in D_{nh} M_nN_nSi complexes (M = transition-metals; N = H, Cl; $n = 4, 5, 6$) [21,22].

To investigate the thermodynamic stabilities of the D_{4h} Ni_4Cl_4X complexes relative to free D_{4h} Ni_4Cl_4 ligands and X atoms (X = C, Si, Ge), the thermodynamic quantity changes of the following reactions:

$$Ni_4Cl_4(D_{4h}) + X = Ni_4Cl_4X(D_{4h})$$

have been calculated at DFT level, with the energy changes of $\Delta E = -778.8$, -571.9, -475.1 kJ/mol, enthalpy changes of $\Delta H = -783.9$, -574.1, -476.2 kJ/mol, and Gibbs energy changes of $\Delta G = -732.8$, -528.7, -430.5 kJ/mol for X = C, Si, and Ge, respectively. The perfectly squared Ni_4Cl_4X complexes with ptC, ptSi, and ptGe centers are clearly favored in thermodynamics with respect to free Ni_4Cl_4 and X. Dynamic investigation on these processes requires much more powerful computing capacities which are out the reach of available resources.

For neutral Ni_4Cl_4X complexes (X = C, Si, Ge), the calculated negative HOMO energies (<−6.27 eV), the big HOMO–LUMO energy gaps (>2.46 eV), and high IP values (>6.852 eV) further support their stabilities (see Table 1). The calculated VDEs of the $Ni_4Cl_4X^-$ anions are 3.161, 2.308, and 1.958 eV for X = B, Al, Ga, respectively, well in line with the decreasing electronegativities of the

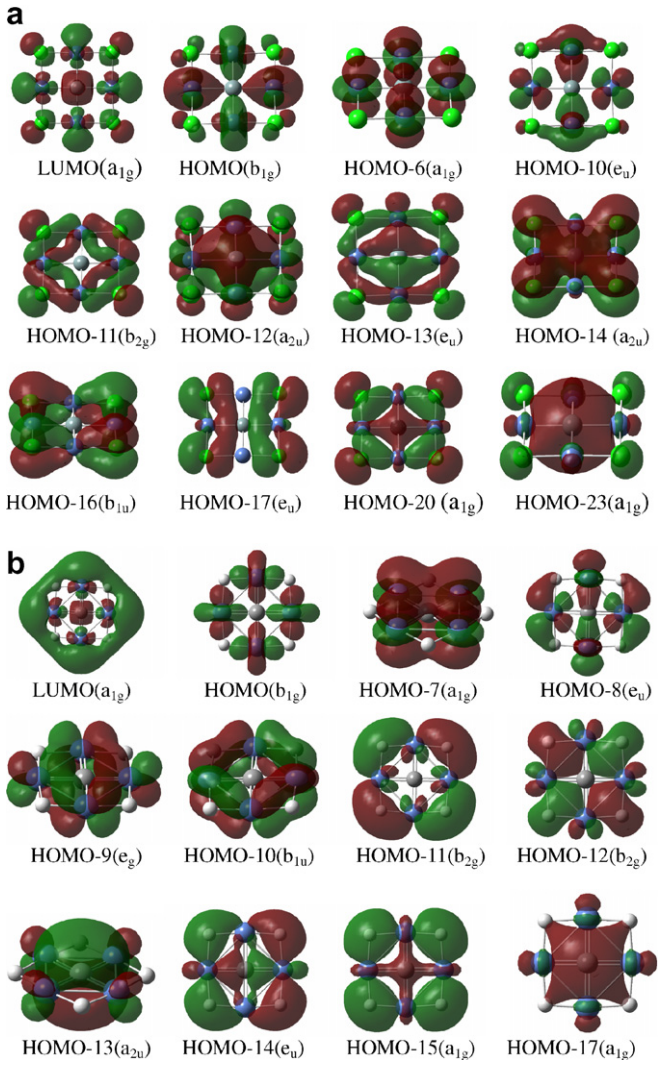

Fig. 3. Comparison of the LUMO, HOMO, and typical delocalized δ, π, and σ molecular orbitals of D_{4h} Ni_4Cl_4Si (a) and D_{4h} Ni_4H_4C (b). For doubly degenerate MOs, only one of them is depicted.

ptX centers from B, Al to Ga. The DFT values obtained above may facilitate future photo-electron spectroscopy measurements to confirm these novel complexes.

NBO analyses indicate that the ptX centers in M_4Cl_4X series (M = Ni, Pd, Pt; X = C, Si, Ge) follow the octet rule, with the total Wiberg bond indices varying in the range of $WBI_X = 3.22–3.79$. The bond orders of individual bonds turn out to be $WBI_{Ni–X} = 0.68–0.80$, $WBI_{Ni–Cl} = 0.35–0.36$, and $WBI_{Ni–Ni} = 0.12–0.19$ in Ni_4Cl_4X series (X = Ge, Si, C). These values confirm the existence of the Ni—X single bonds, the Ni—Cl—Ni bridging bonds, and the weak d–d interactions between neighboring Ni atoms. There also exist delocalized multi-center bonds in these systems which have not been included in our NBO calculations. The natural atomic charge distribution of D_{4h} Ni_4Cl_4Si turned out to be Si +0.36 |e|, Ni +0.40 |e|, and Cl −0.49 |e|, corresponding to the atomic electron configurations of $Si[Ne]3s^{1.47}3p_x^{0.85}3p_y^{0.85}3p_z^{0.40}$, $Ni[Ar]4s^{0.36}3d_{xy}^{1.98}3d_{xz}^{1.99}3d_{yz}^{1.90}3d_{x^2-y^2}^{1.38}3d_{z^2}^{1.96}$, and $Cl[Ne]3s^{1.91}3p_x^{1.78}3p_y^{1.78}3p_z^{1.98}$, respectively. Similar situation occurs to D_{4h} Ni_4Cl_4Ge. Obviously, Si and Ge centers and Ni ligands in these complexes carry positive charges, while the most electronegative Cl bridges possess negative charges. However, the D_{4h} ptC center in D_{4h} Ni_4Cl_4C possesses the negative charge of −0.45 |e| which corresponds to the electron configuration of $C[He]2s^{1.52}3p_x^{1.10}3p_y^{1.10}3p_z^{0.68}$. This is similar to the situation in D_{4h} Ni_4H_4C[11], in which C carries the natural charge of −0.55 |e| and has the electron configuration of $[He]2s^{1.49}2p_x^{1.16}2p_y^{1.16}2p_z^{0.68}$.

Orbital analyses of the prototype D_{4h} Ni_4Cl_4Si help to understand the bonding patterns in these complexes (see Fig. 3a and Supporting Information). The LUMO (a_{1g}) of Ni_4Cl_4Si is an anti-bonding MO mainly between $Ni3d_{x^2-y^2}$ and Si 3s, while HOMO (b_{1g}) appears to be a partially bonding MO mainly between $Ni3d_{x^2-y^2}$ orbitals. Among the typical delocalized bonding MOs of D_{4h} Ni_4Cl_4Si, HOMO-6(a_{1g}) is a bonding d–d δ–MO between the four $Ni3d_{z^2}$ orbitals perpendicular to the molecular plane (with minor contributions from Si 3s), HOMO-12(a_{2u}) is a strong bonding d–p π–MO between Si $3p_z$ and Ni $3d_{xz}$ (or $3d_{yz}$), while HOMO-14 (a_{2u}) proves to be a bonding p–p π–MO mainly consisting of the in-phase overlap between the four Cl $3p_z$ orbitals (with minor contribution from Si $3p_z$). The degenerate HOMO-10(e_u) and HOMO-13(e_u) reflect the σ-bonding between Si—Ni. HOMO-11(b_{2g}), HOMO-13(e_u), HOMO-17(e_u), and HOMO-20(a_{1g}) turn out to be delocalized p–d σ–MOs mainly representing the Ni—Cl—Ni bridging interactions. HOMO-16(b_{1u}) appears to be a delocalized p–d π–MO between Ni $3d_{xz}$ (or $3d_{yz}$) and Cl $3p_z$ orbitals perpendicular to the molecular plane, while HOMO-23(a_{1g}) is basically a long pair MO from Si 3s. The delocalized MOs discussed above create extra multiple bonding effects to effectively stabilize the systems. D_{4h} Ni_4Cl_4Ge has similar delocalized MOs with D_{4h} Ni_4Cl_4Si. D_{4h} Ni_4Cl_4C, which contains a more electronegative ptC center than both ptSi and ptGe, possesses roughly a similar bonding pattern with D_{4h} Ni_4Cl_4Si with a different MO energy order. The Ni–Ni distances in Ni_4Cl_4C are 0.47 Å shorter than that in Ni_4Cl_4Si. This bond length shortening causes the delocalized π and δ interactions of Ni_4Cl_4C to be more densely concentrated on ptC at the square center. HOMO-8(a_{1g}), HOMO-16(a_{2u}), and HOMO-19(a_{2u}) of Ni_4Cl_4C are typical such interactions (see Supporting Information). The electronegativity difference between Si and C results in the charge distribution difference in M_4Cl_4X complexes (see Tables 1 and 2).

A comparison of the MOs of Ni_4H_4C (b) with Ni_4Cl_4Si (a) in Fig. 3 would reveal the bonding pattern difference between them. The delocalized δ-typed HOMO-7(a_{1g}) of Ni_4H_4C exhibits more effective orbital overlap between Ni $3d_{z^2}$ than that in the corresponding HOMO-6(a_{1g}) of Ni_4Cl_4Si. The π-typed HOMO-13(a_{2u}) of Ni_4H_4C contains more contribution from C $2p_z$ than that in the HOMO-12(a_{2u}) from Si $3p_z$. The much shorter Ni–Ni distance of 2.469 Å in Ni_4H_4C [11] leads to the formation of the δ-typed HOMO-9(e_g) and HOMO-10(b_{1u}) between Ni $3d_{xz}$

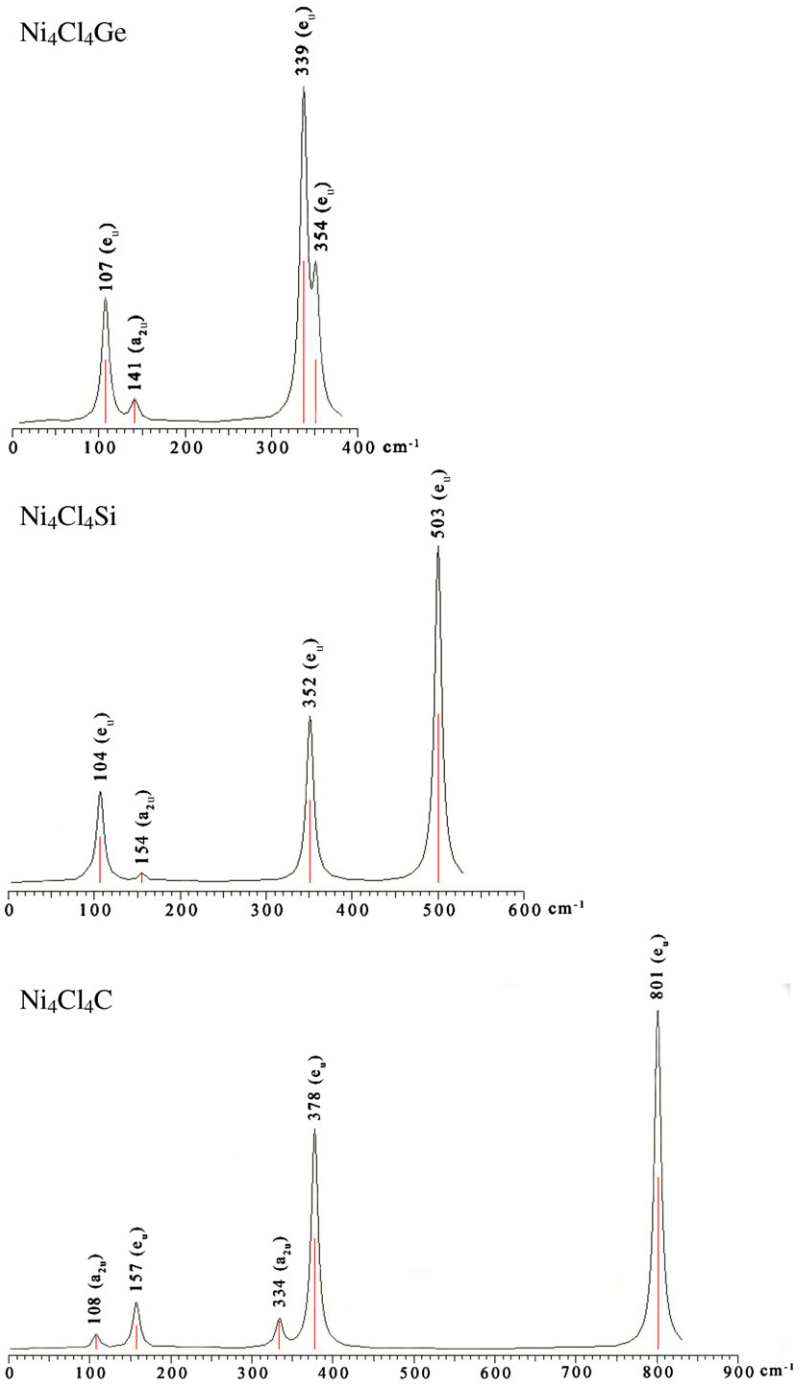

Fig. 4. Comparison of the calculated IR spectra of D_{4h} Ni_4Cl_4Ge, Ni_4Cl_4Si, and D_{4h} Ni_4Cl_4C.

(or $3d_{yz}$). There are no such interactions in Ni_4Cl_4Si which has the much longer Ni–Ni distances of 3.010 Å. As discussed above, the Ni—Cl—Ni bridging bonding in Ni_4Cl_4Si contains contributions from both the in-plane σ- and off-planed π-typed bonds between Cl 3p and Ni 3d, while in Ni_4H_4C, the corresponding MOs of HOMO-11(b_{2g}), HOMO-12(b_{2g}), HOMO-14(e_u), and HOMO-15(a_{1g}) mainly represent the in-plane σ-typed bridging bonding between H 1s and Ni 3d. The delocalized π-typed HOMO-14(a_{2u}) of Ni_4Cl_4Si, which represents the off-planed overlap between Cl $3p_z$ orbitals, finds no counterpart in Ni_4H_4C. Cl atoms in Ni_4Cl_4Si form both σ- and π-typed bridging bonds with neighboring Ni atoms, while H bridges in Ni_4H_4C only participate in σ-typed Ni—H—Ni interactions.

As shown in Fig. 4, the first three IR active vibrational modes of D_{4h} Ni_4Cl_4Si at 104 cm^{-1}(e_u), 154 cm^{-1}(a_{2u}), and 352 cm^{-1}(e_u) have been kept almost unchanged in both D_{4h} Ni_4Cl_4Ge and D_{4h} Ni_4Cl_4C (For D_{4h} Ni_4Cl_4C, the first two vibrational modes at 108 cm^{-1}(a_{2u}) and 157 cm^{-1}(e_u) have exchanged in energy order). Here, the two e_u modes mainly involve the in-plane vibrations of the four Ni atoms in the

Table 1
Optimized bond lengths (r/Å), calculated natural charges (q_x/|e|) and total Wiberg bond indices (WBI_X) of the central atoms, the lowest vibration frequencies (ν_{min}/cm^{-1}), HOMO energies (E_{HOMO}/eV), and HOMO–LUMO energy gaps (ΔE_{gap}/eV) of Ni_4Cl_4X complexes (X = C, Si, Ge, B, Al, Ga, N, P, As) at B3LYP/6-311 + G(3df) level

	State	Symmetry	r_{X-Ni}	R_{Ni-Cl}	R_{Ni-Ni}	q_x	ν_{min}	WBI_X	E_{HOMO}	ΔE_{gap}	VDE
Ni_4Cl_4	$^3A_{1g}$	D_{4h}		2.145	2.344		−7 (b_{2u})		−7.49	2.52	
Ni_4Cl_4C	$^1A_{1g}$	D_{4h}	1.795	2.191	2.538	−0.45	+32 (b_{1u})	3.68	−6.98	2.74	7.571
Ni_4Cl_4Si	$^1A_{1g}$	D_{4h}	2.129	2.192	3.010	+0.36	+30 (b_{1u})	3.50	−6.50	2.80	7.273
Ni_4Cl_4Ge	$^1A_{1g}$	D_{4h}	2.210	2.201	3.125	+0.31	+36 (b_{1u})	3.35	−6.27	2.46	6.852
$Ni_4Cl_4B^-$	$^1A_{1g}$	D_{4h}	1.870	2.200	2.644	−0.20	+30 (b_{1u})	3.49	−1.93	2.83	3.161
$Ni_4Cl_4Al^-$	$^1A_{1g}$	D_{4h}	2.233	2.200	3.158	+0.46	+33 (b_{1u})	2.98	−1.73	2.91	2.308
$Ni_4Cl_4Ga^-$	$^1A_{1g}$	D_{4h}	2.258	2.209	3.194	+0.29	+26 (b_{1u})	2.89	−1.63	2.55	1.958
$Ni_4Cl_4N^+$	$^1A_1$	C_{2v}	1.788	2.187	2.564	−0.78	+27 (a_2)	3.15	−12.19	2.47	
$Ni_4Cl_4P^+$	$^1A_{1g}$	D_{4h}	2.075	2.186	2.934	+0.15	+29 (b_{1u})	3.61	−11.51	2.48	
$Ni_4Cl_4As^+$	$^1A_{1g}$	D_{4h}	2.187	2.196	3.093	+0.22	+37 (b_{1u})	3.47	−11.14	2.13	

The first vertical one-electron detachment energies (VDE/eV) of the neutrals and anions are also presented at OVGF/B3LYP/6-311 + G(3df).

Table 2
Optimized bond lengths (r/Å), calculated natural charges (q_x/|e|) and total Wiberg bond indices (WBI_X) of the central atoms, the lowest vibration frequencies (ν_{min}/cm^{-1}), HOMO energies (E_{HOMO}/eV), and HOMO–LUMO energy gaps (ΔE_{gap}/eV) of M_4Cl_4X complexes (M = Pd, Pt; X = C, Si, Ge) at B3LYP/6-311+G(d)/Lanl2dz level

	State	Symmetry	r_{X-M}	R_{M-Cl}	R_{M-M}	q_x	ν_{min}	WBI_X	E_{HOMO}	ΔE_{gap}
Pd_4Cl_4	$^3A_{1g}$	D_{4h}		2.395	2.625		+22		−7.99	2.27
Pd_4Cl_4C	$^1A_{1g}$	D_{4h}	1.963	2.436	2.776	−0.32	+22	3.63	−7.44	2.18
Pd_4Cl_4Si	$^1A_{1g}$	D_{4h}	2.256	2.419	3.190	+0.52	+35	3.39	−7.56	2.80
Pd_4Cl_4Ge	$^1A_{1g}$	D_{4h}	2.349	2.422	3.322	+0.46	+45	3.22	−7.42	2.51
Pt_4Cl_4	$^3A_{1g}$	D_{4h}		2.398	2.622		−33		−7.79	2.77
Pt_4Cl_4C	$^1A_{1g}$	D_{2d}	1.993	2.439	2.818	−0.43	+23	3.79	−6.71	1.97
Pt_4Cl_4Si	$^1A_{1g}$	D_{2d}	2.295	2.392	3.245	+0.52	+48	3.63	−7.14	2.93
Pt_4Cl_4Ge	$^1A_{1g}$	D_{4h}	2.374	2.399	3.357	+0.49	+21	3.47	−7.06	2.59

Ni_4Cl_4 ligand and the a_{2u} mode the off-planed movements of the central atom X. However, the fourth peak (e_u) turns out to be dramatically changed in vibration energies with different planar coordinated centers: it increases from 354 cm^{-1} for Ni_4Cl_4Ge, 503 cm^{-1} for Ni_4Cl_4Si, to 801 cm^{-1} for Ni_4Cl_4C. Frequency analyses indicate that the last peaks in these IR spectra all correspond to two degenerate vibrational modes of the central atom (e_u modes) which mainly involve the in-plane stretching vibrations of the Ni—X bonds in perpendicular directions. This increasing energy order well reflects the bond-strength increasing from Ge—Ni, Si—Ni, to C—Ni.

Analogous to D_{4h} Ni_4Cl_4Si, both Pd_4Cl_4X and Pt_4Cl_4X series (X = C, Si, Ge) take perfectly (D_{4h}) or slightly distorted (D_{2d}) squared ground-state structures with slightly longer bond lengths (see Table 2). These second- and third-row transition metal complexes have the HOMO energies lower than −6.71 eV and HOMO–LUMO gaps wider than 1.97 eV. Their planar tertra-coordinate centers X possess the natural charges (q_x) and bond orders similar to the corresponding values of Ni_4Cl_4X series. Obviously, PtC, ptSi, and ptGe centers are stabilized in heavy transition metal complexes M_4Cl_4X (M = Pd and Pt) in bonding patterns similar to D_{4h} Ni_4Cl_4Si.

A D_{2h} $Ni_6Cl_6Si_2$ (**4**) chain containing double ptSi centers has also been confirmed o be a true minimum at DFT. Structure **4** proves to have similar bond parameters and bond orders with **3** (see Fig. 1). Concerning its thermodynamic stability, the following reaction $2Ni_4Cl_4(D_{4h}) + 2\text{-}Si = Ni_6Cl_6Si_2(D_{2h}) + Ni_2Cl_2(D_{2h})$ possesses the thermodynamic quantity changes of $\Delta E = -981.1$ kJ/mol, $\Delta H = -984.00$ kJ/mol, and $\Delta G = -902.4$ kJ/mol (the ground-state of Ni_2Cl_2 is a triplet rhombus). D_{2h} $Ni_6Cl_6Si_2$ may be further extended to form C_{2v} $Ni_{2n+2}Cl_{2n+2}Si_n$ chains with multiple ptSi centers.

4. Summary

DFT investigations performed in this work indicate that a wide range of planar tetra-coordinate inorganic atoms can be stabilized at the centers of the perfectly squared M_4Cl_4 ligands to form planar or quasi-planar M_4Cl_4X complexes (M = Ni, Pd, Pt; X = C, Si, Ge, B, Al, Ga, N, P, As). The results obtained in this work provide a general pattern to coordinate planar tetra-coordinate inorganic atoms with transition metal ligands. Delocalized δ, π and σ molecular orbitals introduce extra stabilizing energies to these novel structures. Our previous investigations [21,22] and the current work complete the series of planar coordinate silicon and germanium with the highest symmetries of D_{4h}, D_{5h}, and D_{6h}.

Acknowledgement

This work was jointly supported by the Natural Science Foundation of China (No. 20573088) and Shanxi Natural Science Foundation (No. 2006011024).

Appendix A. Supplementary data

Supplementary data associated with this article can be found, in the online version, at doi:10.1016/j.theochem.2007.03.040.

References

[1] R. Hoffmann, R.W. Alder, C.F. Wilcox Jr., J. Am. Chem. Soc. 92 (1970) 4992.
[2] X. Li, L.-S. Wang, A.I. Boldyrev, J. Simons, J. Am. Chem. Soc. 121 (1999) 6033.
[3] L.-S. Wang, A.I. Boldyrev, X. Li, J. Simons, J. Am. Chem. Soc. 122 (2000) 7681.
[4] X. Li, H.-J. Zhai, L.-S. Wang, Chem. Phys. Lett. 357 (2002) 415.
[5] X. Li, H.-F. Zhang, L.-S. Wang, G.D. Geske, A.I. Boldyrev, Angew. Chem. Int. Ed. 39 (2000) 3630.
[6] Z.-X. Wang, P.v.R. Schleyer, J. Am. Chem. Soc. 123 (2001) 994.
[7] K. Sorger, P.v.R. Schleyer, J. Mol. Struct. 338 (1995) 317.
[8] G. Merino, M.A. Mendez-Rojas, A. Vela, J. Am. Chem. Soc. 125 (2003) 6026.
[9] P.M. Esteves, N.B.P. Ferreira, R.J. Correa, J. Am. Chem. Soc. 127 (2005) 8680.
[10] R.M. Minyaev, T.N. Gribanova, V.I. Minkin, A.G. Starikov, R. Hoffmann, J. Org. Chem. 70 (2005) 6693.
[11] S.-D. Li, G.-M. Ren, C.-Q. Miao, Z.-H. Jin, Angew. Chem. Int. Ed. 43 (2004) 1371.
[12] S.-D. Li, G.-M. Ren, C.-Q. Miao, J. Phys. Chem. A 109 (2005) 259.
[13] D. Roy, C. Corminboeuf, C.S. Wannere, R.B. King, P.v.R. Schleyer, Inorg. Chem. 45 (2006) 8902.
[14] Z.-X. Wang, P.v.R. Schleyer, Science 292 (2001) 2465.
[15] K. Exner, P.v.R. Schleyer, Science 290 (2000) 1937.
[16] (a) H. Meyer, G. Nagorsen, Angew. Chem. Int. Ed. Engl. 18 (1979) 554;
(b) E.U. Wurthwein, P.v.R. Schlyer, Angew. Chem. Int. Ed. Engl. 18 (1979) 553.
[17] (a) A.I. Boldyrev, X. Li, L.-S. Wang, Angew. Chem. Int. Ed. 39 (2000) 3307;
(b) A.I. Boldyrev, L.-S. Wang, J. Phys. Chem. A 105 (2001) 10759.
[18] (a) P. Belanzoni, G. Giorgi, G.F. Cerofolini, Chem. Phys. Lett. 418 (2006) 383;
(b) P. Belanzoni, G. Giorgi, G.F. Cerofolini, A. Sgamellotti, J. Phys. Chem. A 110 (2006) 4582;
(c) P. Belanzoni, G. Giorgi, G.F. Cerofolini, A. Sgamellotti, Theor. Chem. Acc. 115 (2006) 448.
[19] S.-D. Li, C.-Q. Miao, J.-C. Guo, G.-M. Ren, J. Am. Chem. Soc. 126 (2004) 16227.
[20] S.-D. Li, J.-C. Guo, C.-Q. Miao, G.-M. Ren, J. Phys. Chem. A 109 (2005) 4133.
[21] S.-D. Li, C.-Q. Miao, J. Phys. Chem. A 109 (2005) 7594.
[22] S.-D. Li, G.-M. Ren, C.-Q. Miao, Inorg. Chem. 43 (2004) 6331.
[23] (a) A.D. Becke, J. Chem. Phys. 98 (1993) 5648;
(b) C. Lee, W. Yang, R.G. Parr, Phys. Rev. B 37 (1988) 785.
[24] M.J. Frisch et al., Gaussian 03, Revision A.1, Gaussian, Inc., Pittsburgh, PA, 2003.
[25] (a) P.J. Hay, W.R. Wadt, J. Chem. Phys. 82 (1985) 270;
(b) W.R. Wadt, P.J. Hay, J. Chem. Phys. 82 (1985) 284;
(c) P.J. Hay, W.R. Wadt, J. Chem. Phys. 82 (1985) 299.
[26] (a) J.V. Ortiz, J. Chem. Phys. 89 (1988) 6348;
(b) V.G. Zakrzewski, W. von Niessen, J. Comp. Chem. 14 (1993) 13;
(c) V.G. Zakrzewski, J.V. Ortiz, Int. J. Quant. Chem. 53 (1995) 583;
(d) J.V. Ortiz, Int. J. Quant. Chem. Symp. 22 (1988) 431;
(e) W. von Niessen, J. Schirmer, L.S. Cederbaum, Comp. Phys. Rep. 1 (1984) 57.